

Compact and scalable three-dimensional microelectromechanical system optical switches [Invited]

Volkan Kaman, Roger J. Helkey, and John E. Bowers

Calient Networks, 25 Castilian Drive, Goleta, California 93117, USA
 vkaman@calient.net

Received August 21, 2006; accepted October 1, 2006; published December 13, 2006 (Doc. ID 74237)

We review the performance and applications of compact (20 cm³) and large-scale (320×320) three-dimensional microelectromechanical system (3-D MEMS) based optical switches. The low loss (<3 dB for all 102,400 paths) and variable attenuation capable optical switch performs penalty-free for cascaded operation at 40 Gbits/s. Scalability and performance of integrated wavelength-selective cross-connects based on 3-D MEMS with an unprecedented 12.8 Tbit/s switching capacity for next-generation all-optical networks are also presented. © 2006 Optical Society of America
 OCIS codes: 060.0060, 130.0130.

1. Introduction

With the rapid deployment of passive optical networks (PONs) and triple-play services, a number of network operation challenges, such as fiber management, fiber fault localization, and customer churn, have emerged from the growing outside-plant fiber infrastructure [1]. A remotely managed automated fiber solution based on large-scale optical switches with small footprint and low power consumption is a good candidate to address these challenges and adds further value by integrating remote test and monitoring capabilities for fast and precise fault isolation [2]. As an automated patch panel, a large-scale optical switch is also desirable in lab automation applications in which testing accuracy and speed are critical. While optical switches based on InP [3] or 2-D microelectromechanical systems (MEMSs) [4] have been demonstrated, these technologies do not scale beyond 16 to 32 ports, as the optical loss increases dramatically. On the other hand, compact optical switches with greater than 300 ports and low loss have been demonstrated using scalable 3-D MEMS [5,6]. The wide wavelength range (1250 to 1650 nm) of operation of these 3-D MEMS switches is particularly ideal for the above-mentioned applications, where low loss in several bands of the spectrum is critical (for example, in PONs, the upstream wavelength is 1310 nm, downstream wavelength is 1490 nm, the video overlay wavelength is 1550 nm, and the fault localization wavelength is 1625 nm).

The growth in access networks also leads to larger capacity requirements in metropolitan, regional, and long-haul networks, which require photonic cross-connect nodes that can support multiple dense wavelength division multiplexed (DWDM) channels at fast bit rates [7]. As large-scale electronic switching is limited beyond 10 Gbits/s and also has additional drawbacks such as high power consumption and large rack space, next-generation reconfigurable optical networks based on future-proof all-optical switching nodes become an attractive alternative. Integrated and ultracompact wavelength-selective photonic cross-connects (WSPXCs) based on large-scale and bit-rate transparent 3-D MEMS optical switches provide dynamic wavelength switching of multiple degrees of fiber, support for 100% add-drop without incurring any excess loss penalty, and inherent per-channel power balancing, are thus the leading candidate for the next-generation DWDM switching node [8–10].

In this paper, we review the performance of a bit-rate and wavelength transparent compact 320×320 optical switch based on 3-D MEMS. In Section 2, we describe the static optical switch performance, which includes optical insertion loss, wavelength-dependent loss (WDL), polarization-dependent loss (PDL), and cross talk. In Section 3, we present the dynamic optical switch characteristics that include 40 Gbit/s cascability performance and variable attenuation by mirror detuning. Finally, in

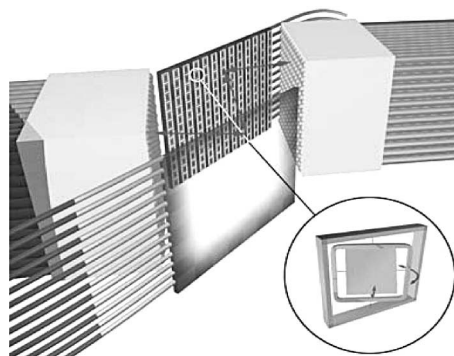


Fig. 1. Schematic layout of the compact 3-D MEMS optical switch.

Section 4, we discuss the scalability of WSPXCs based on 3-D MEMS switches and review their performance.

2. Static Optical Switch Performance

The schematic layout of the 3-D MEMS optical switch, which consists of two pairs of fiber arrays and two pairs of MEMS mirror arrays, is shown in Fig. 1. A low-loss light path is established from an input fiber to an output fiber by collimating the beam by a lens onto the MEMS mirror [5]. This input mirror then steers the beam onto the other MEMS array, where an output mirror points to the desired output fiber. This optical switch scales to greater than 300 ports in a compact volume of 20 cm^3 that includes the two fiber array blocks and the MEMS mirror arrays.

The optical loss distribution measured at 1310 nm for the 320×320 optical switch is shown in Fig. 2(a). All 102,400 paths achieve a measured loss of less than 2.9 dB with a median loss of 1.4 dB. It should be emphasized that these measurements include additional loss and uncertainty errors due to multifiber connectors (used for ease of testing), which results in the widening of the expected core switch loss distribution and therefore in an increase of the expected maximum loss of 2 dB [5]. The WDL performance of the optical switch for a typical path is shown in Fig. 2(b) with a less than 0.5 dB variation over the entire 1250 to 1650 nm range.

The measured median PDL of the optical switch at 1550 nm is less than 0.1 dB with a maximum of 0.3 dB. Chromatic dispersion ($<0.5 \text{ ps/nm}$) and polarization-mode dispersion ($<10 \text{ fs}$) are negligible, and degradation of signal quality beyond 40 Gbits/s is not expected. The measured switch return loss for all ports is better than 40 dB, while optical cross talk is less than -60 dB . It should be noted that cross talk is primarily dominated by adjacent ports, while the contribution from other ports is typically less than -80 dB . The excellent optical properties of 3-D MEMS optical switches allow for a transparent introduction of these large-scale switches into various applications in PON networks, lab automation, and DWDM all-optical networks.

3. Dynamic Optical Switch Performance

The cascadability of the 3-D MEMS optical switches was characterized at 10 and 40 Gbits/s. It was previously demonstrated in a 10 Gbit/s recirculating loop testbed

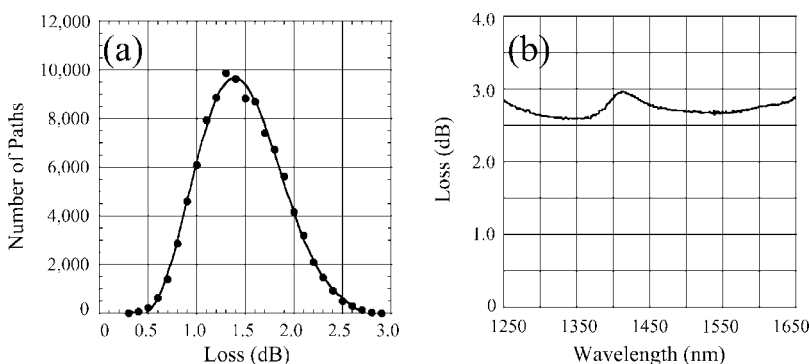


Fig. 2. (a) Loss distribution and (b) WDL response of the 3-D MEMS optical switch.

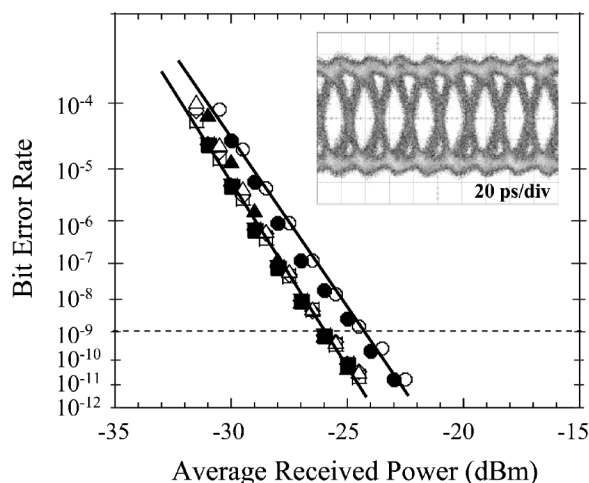


Fig. 3. 40 Gbit/s BER measurements with no switch (filled circles) and 18 cascaded switch paths (open circles). Inset, received 40 Gbit/s eye diagram.

that the optical switch introduces less than 0.5 and 1.7 dB penalties after 20 and 60 transitions through the switch, respectively, due to incremental accumulation of PDL [8].

Figure 3 shows the bit error rate (BER) measurements at 40 Gbits/s for all four tributary channels with no switch and after cascading 18 switch paths. No significant power penalty was observed with the cascaded switch paths, and the inset to Fig. 3 shows the open 40 Gbit/s eye diagram at the receiver. Since next-generation all-optical DWDM networks are not expected to exceed 10–15 switching node transitions, the lack of significant signal degradation at bit rates of 40 Gbits/s reconfirm the transparent nature of 3-D MEMS optical switches as discussed in Section 2.

An advantageous feature of 3-D MEMS optical switches is their ability to detune mirrors to induce variable attenuation on optical signals [10]. This inherent characteristic of 3-D MEMS eliminates the need for external variable optical attenuators in various applications such as DWDM power balancing and amplified spontaneous emission noise suppression, which reduces the size, cost, power consumption, and additional optical loss. Attenuation levels up to 20 dB can be achieved with minimal disturbance on the optical stability and cross talk by simultaneously attenuating both the input and output mirrors. Figure 4 shows the BER measurements comparing no switch and four cascaded and attenuated switch paths. After inducing 12 dB attenuation on each of two high-angle paths and 5 and 13 dB attenuation on two low-angle paths, the measured receiver sensitivity at a BER of 10^{-9} is within 0.3 dB of the baseline without the switch. Figure 5 shows less than 4 ms fall and rise times for a typical switch path when 10 dB attenuation is applied and reversed.

4. Wavelength-Selective Photonic Cross-Connect

Next-generation ultrahigh-capacity mesh optical networks will require wavelength-selective cross-connects (WSXCs) with high throughput and large add-drop capability

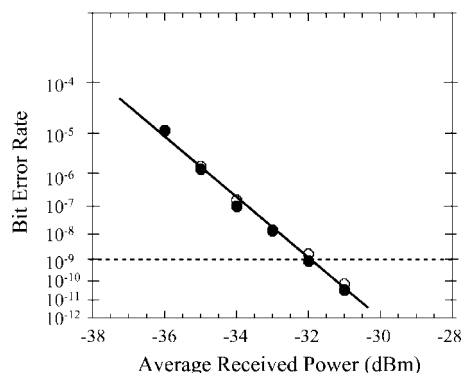


Fig. 4. BER measurements with no switch (filled circles) and four detuned switch paths (open circles).

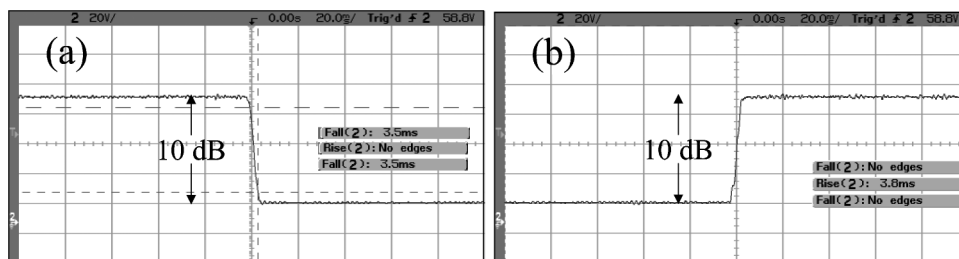


Fig. 5. (a) Fall (3.5 ms) and (b) rise times (3.8 ms) for 10 dB attenuation.

that will enable dynamic reconfigurability and provide end-to-end network-level protection and restoration [7]. Therefore, the WSXC node must be scalable and modular to support up to eight degrees (fibers) and 100% add-drop (with typical 20–30% ratios, including regeneration and wavelength conversion). The WSXC also needs to allow each tunable add-drop transponder to have seamless and colorless access to all N fibers of the node to provide the dynamic end-to-end mesh protection and restoration feature of the network. As will be described in this Section, ultracompact integrated WSPXCs based on 3-D MEMS optical switches fulfill the aforementioned requirements of next-generation high-capacity WSXC nodes.

The WSPXC is shown schematically in Fig. 6. An incoming-outgoing DWDM signal is de/multiplexed into granular wavelengths using an array-waveguide grating (AWG) or thin-film filter (TFF) based de/multiplexers (D/MUXs). At the core of the WSPXC is the 320×320 nonblocking 3-D MEMS optical switch that directs each individual wavelength to any of the desired fiber outputs. Tunable add-drop transponders directly access the core switch and can be directed to any of the desired input-output fibers due to the nonblocking and colorless switching ability of the core switch. Similarly, the access over the full optical band allows for wavelength-resource sharing (wavelength converters and regenerators) at the WSPXC, which reduces the network level cost and increases efficiency. An ultracompact (20 cm^3) WSPXC can be realized by integrating AWG D/MUXs directly into the fiber block arrays (Fig. 1) with an unprecedented capacity of up to 12.8 Tbits/s at a 40 Gbit/s data rate. Alternatively, the WSPXC can also be configured to provide up to 100% add-drop without incurring any extra optical loss.

A WSXC node can also be realized by using a broadcast-and-select architecture based on wavelength blockers and passive optical splitters [11]; however, this architecture scales poorly due to unacceptable high optical losses as the node degree and/or the add-drop ratio increase. An alternative architecture is based on 1:K wavelength-selective switches (WSSs) that distribute the incoming DWDM channels to any of the K outputs (with typical $K \leq 9$) [12]. A two-degree reconfigurable optical add-drop multiplexer (ROADM) is realized by cascading either two WSSs or one WSS and a passive coupler [13]. The ROADM modules can then be interconnected for an N -degree WSXC node. In this architecture, the ROADM modules can only provide direct add-drop for a very limited number of transponders ($K-N$); therefore, D/MUXs followed by optical switches are required at each add-drop. The size of the required optical switch is

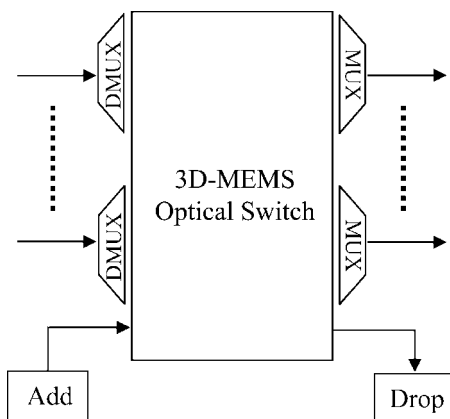


Fig. 6. Schematic of 3-D MEMS based WSPXC.

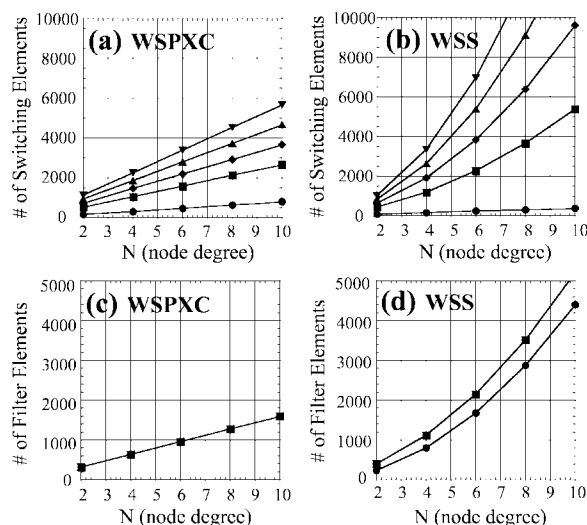


Fig. 7. (a), (b) Scalability of switching and (c), (d) filter elements as a function of node degree and add-drop ratio (circles, squares, diamonds, upper and lower triangles are 0, 0.25, 0.5, 0.75 and 1 add-drop, respectively).

determined by the number of wavelengths on the D/MUX, the number of anticipated transponders, and the degree of the node, adding complexity and loss to the WSXC node. The direct and colorless add-drop access ability of the WSPXC is one of the most significant features differentiating the 3-D MEMS based WSPXC from the other WSXC architectures.

Figure 7 compares the number of switching [Figs. 7(a) and 7(b)] and filtering [Figs. 7(c) and 7(d)] elements in the WSXC node as the node degree and the add-drop ratio are increased. The WSPXC node architecture uses two 3-D MEMS switch cores for protection, while the WSS based architecture assumes a ROADM module based on a single (1-D MEMS) WSS with passive couplers. While the WSPXC architecture elements show a linear relationship with the node degree as the number of add-drops is increased, the number of WSS architecture elements increase quadratically, which clearly shows that the WSPXC is a more scalable and cost-effective architecture for increasing node degrees and add-drop ratios, while the WSS architecture is advantageous for \leq three-degree nodes and a low number of add-drops. The optical insertion loss for add-drop and express paths in an integrated WSPXC can vary between 6 to 8 dB and 9 to 13 dB, respectively, depending on the desired spectral shape of the D/MUXs as determined by the number of WSXC node transitions required in the network. On the other hand, the WSS ROADM architecture add-drop loss is higher due to the additional components, while the express loss is comparable to that of the WSPXC.

The performance of a WSPXC was recently successfully evaluated in a 10 Gbit/s recirculating loop testbed with 8 WSPXC transitions and 600 km single-mode fiber (SMF) [8] and 10 WSPXC transitions and 400 km SMF [9]. Figure 8 shows the

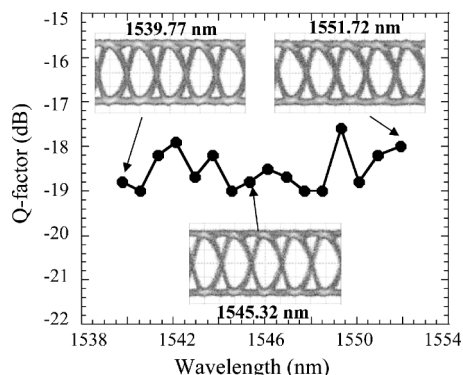


Fig. 8. Q-factors after 8 WSPXC transitions and 600 km SMF fiber [8].

received eye diagrams and the measured Q -factors with all channels performing better than 17 dB.

5. Conclusions

In this paper, we reviewed the performance and applications of compact and integrated 3-D MEMS based optical switches. The excellent optical properties of the 320×320 switch with negligible 40 Gbit/s signal degradation and inherent attenuation capability, together with its small size and remote control, makes it an ideal candidate for a variety of fiber-rich applications in access and next-generation all-optical mesh networks. As an integrated wavelength-selective switching node, a 3-D MEMS based WSPXC architecture with 12.8 Tbit/s capacity was shown to be the optimum choice for high degree nodes and add-drop ratios.

References and Links

1. H. Shinohara, "NTT's deployment of FTTH services," in *Optical Fiber Communication Conference (OFC 2004)* (Optical Society of America, 2004), Vol. 2, paper ThW2.
2. P. Thomson and R. Mackey, "Addressing profitability issues in FTTP network management," *Lightwave* **23**, 1–36 (2006).
3. R. Varrazza, T. Bricheno, and S. Yu, "A fully packaged 4×4 integrated optical switch matrix," *IEEE J. Sel. Top. Quantum Electron.* **11**, 1248–1254 (2005).
4. L. Y. Lin, E. L. Goldstein, and R. W. Tkach, "Free-space micromachined optical switches for optical networking," *IEEE J. Sel. Top. Quantum Electron.* **5**, 4–9 (1999).
5. X. Zheng, V. Kaman, S. Yuan, Y. Xu, O. Jerphagnon, A. Keating, R. C. Anderson, H. N. Poulsen, B. Liu, J. R. Sechrist, C. Pularla, R. Helkey, D. J. Blumenthal, and J. E. Bowers, "Three-dimensional MEMS photonic cross-connect switch design and performance," *IEEE J. Sel. Top. Quantum Electron.* **9**, 571–578 (2003).
6. J. Kim, C. J. Nuzman, B. Kumar, D. F. Lieuwen, J. S. Kraus, A. Weiss, C. P. Lichtenwalner, A. R. Papazian, R. E. Frahm, N. R. Basavanhally, D. A. Ramsey, V. A. Aksyuk, F. Pardo, M. E. Simon, V. Lifton, H. B. Chan, M. Haueis, A. Gasparyan, H. R. Shea, S. Arney, C. A. Bolle, P. R. Kolodner, R. Ryf, D. T. Neilson, and J. V. Gates, "1100 \times 1100 port MEMS-based optical crossconnect with 4-dB maximum loss," *IEEE Photon. Technol. Lett.* **15**, 1537–1539 (2003).
7. B. Basch, S. Gringerim, R. Goudreault, and S. Ravukumar, "Evolution of the photonic core within metropolitan and regional networks," in *National Fiber Optical Engineers Conference (NFOEC 2002)*, Vol. 1, pp. 201–207.
8. V. Kaman, X. Zheng, S. Yuan, J. Klingshirn, C. Pularla, R. J. Helkey, O. Jerphagnon, and J. E. Bowers, "Cascadability of large-scale 3-D MEMS-based low-loss photonic cross-connects," *IEEE Photon. Technol. Lett.* **17**, 771–773 (2005).
9. V. Kaman, X. Zheng, S. Yuan, J. Klingshirn, C. Pularla, R. J. Helkey, O. Jerphagnon, and J. E. Bowers, "A 32×10 Gb/s DWDM metropolitan network demonstration using wavelength-selective photonic cross-connects and narrow-band EDFAs," *IEEE Photon. Technol. Lett.* **17**, 1977–1979 (2005).
10. V. Kaman, S. Yuan, J. Klingshirn, X. Zheng, C. Pularla, R. J. Helkey, O. Jerphagnon, and J. E. Bowers, "Optical performance of variable attenuation in large-scale 3-D MEMS-based photonic cross-connects," *IEEE Photon. Technol. Lett.* **17**, 1857–1859 (2005).
11. J.-K. Rhee, I. Tomkos, and M. Li, "A broadcast-and-select OADM optical network with dedicated optical channel protection," *J. Lightwave Technol.* **21**, 25–31 (2003).
12. D. M. Marom, C. R. Doerr, M. Cappuzzo, E. Chen, A. Wong-Foy, and L. Gomez, "Hybrid free-space and planar lightwave circuit wavelength-selective 1×3 switch with integrated drop-side demultiplexer," in *European Conference on Optical Communication (ECOC 2005)* (IEEE, 2005), Vol. 1, pp. 993–994.
13. R. V. Egorov, S. Gringeri, and B. Basch, "DWDM system architecture and design trade-offs," in *National Fiber Optical Engineers Conference (NFOEC)* (Optical Society of America, 2006), Vol. 1, paper NThC2.